HHS Public Access

Author manuscript

Mol Cell. Author manuscript; available in PMC 2018 July 06.

Published in final edited form as:

Mol Cell. 2017 July 06; 67(1): 55–70.e4. doi:10.1016/j.molcel.2017.06.005.

AUTOGENOUS CONTROL OF 5′TOP mRNA STABILITY BY 40S RIBOSOMES

Antonio Gentilella[1,2,*], **Francisco D. Morón-Duran**[1], **Pedro Fuentes**[1,3], **Guilherme Zweig-Rocha**[1], **Ferran Riaño-Canalias**[1], **Joffrey Pelletier**[1], **Marta Ruiz**[1], **Gemma Turón**[1,4], **Julio Castaño**[5], **Albert Tauler**[1,2], **Clara Bueno**[5], **Pablo Menéndez**[5,7], **Sara C. Kozma**[1,8], and **George Thomas**[1,8,*]

[1]Laboratory of Metabolism and Cancer, Catalan Institute of Oncology, ICO, Bellvitge Biomedical Research Institute, IDIBELL, 08908 Barcelona, Spain

[2]Dept. of Biochemistry and Physiology, Faculty of Pharmacy, Universitat de Barcelona, 08028 Barcelona, Spain

[5]Josep Carreras Leukemia Research Institute and School of Medicine, University of Barcelona, Barcelona, Spain

[6]Institut Catala de Recerca i Estudis Avançats (ICREA). Lluis Companys, Barcelona. Spain

[7]Department of Internal Medicine, Division of Hematology/Oncology, University of Cin-cinnati Medical School, Cincinnati, 45267-0508 OH, USA

[8]Departament Ciències Fisiològiques II, Facultat de Medicina, Universitat de Barcelona, 08908, Barcelona, Spain

Abstract

Ribosomal protein (RP) expression in higher eukaryotes is regulated translationally, through the 5′TOP sequence. This mechanism evolved to more rapidly produce RPs on demand in different tissues. Here we show that 40S ribosomes, in a complex with mRNA binding protein LARP1, selectively stabilize 5′TOP mRNAs, with disruption of this complex leading to induction of the impaired ribosome biogenesis checkpoint (IRBC) and p53 stabilization. The importance of this mechanism is underscored in *5q*$^{-}$ syndrome, a macrocytic anemia caused by a large monoallelic deletion, which we found also encompasses the LARP1 gene. Critically, depletion of LARP1 alone in human adult CD34+ bone marrow precursor cells, leads to a reduction in 5′TOP mRNAs

*Correspondence: agentilella@idibell.cat (A.G.), gthomas@idibell.cat (G.T.).

[3]Present Address: Vall d'Hebron Institut de Recerca (VHIR). Department of Surgery and morphological sciences. Universitat Autònoma de Barcelona (UAB), 08035 Barce-lona, Spain.

[4]Present Address: Institute for Research in Biomedicine (IRB), Baldiri Reixac 10, 08028 Barcelona, Spain

Authors Contributions

A. G. and G. T. conceived and designed the study. A.G. performed most of the experiments with F.M.D., G.Z.R., F.R.C., J.P., P.F., M.R. and G.Tu. F.M.D. processed and analyzed RNA-seq and microarray data. C.B. and J.C. carried out lentiviral transductions of CD34+ cells. A.G., A.T., S.C.K, P.M. and G.T. analyzed the data and all the authors provided intellectual support in the discussion of the results. A.G. and G.T. guided the studies and wrote the manuscript.

and the induction of p53. These studies identify a 40S ribosome function, independent of those in translation, which with LARP1 mediates the autogenous control of 5′TOP mRNA stability, whose disruption is implicated in the pathophysiology of *5q*⁻ syndrome.

Graphical Abstract

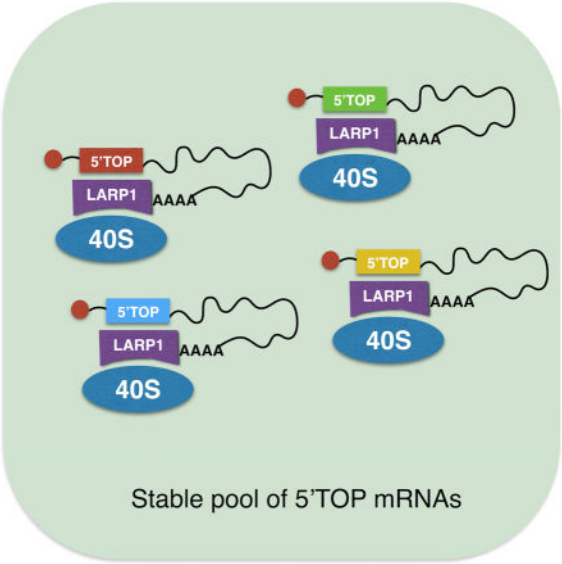

Introduction

Ribosomes are present throughout extant life and are amongst the oldest known molecular machines in cells. From bacteria we have learned a great deal concerning the function of the ribosome, however, the biogenesis of ribosomes is much more complex in eukaryotes, largely confined to the nucleolus (Woolford and Baserga, 2013). In lower eukaryotes, such as yeast, the transcription of ribosomal protein (RP) genes is tightly coordinated with that of rRNA genes (Granneman and Tollervey, 2007). However, in higher eukaryotes the production of RPs is chiefly controlled at the translational level by a 5′-terminal oligopyrimidine (5′TOP) sequence (Gentilella and Thomas, 2012), independent of rRNA production (Pierandrei-Amaldi et al., 1985; Warner, 1977). It is suggested that this evolutionary event developed to more rapidly provide RPs on demand in multicellular organisms (Lam et al., 2007). Importantly, early genetic studies in *Xenopus laevis* revealed a second layer of regulation at the level of RP mRNA stability, proposed to be autonomously controlled by free RPs (Amaldi et al., 1989; Pierandrei-Amaldi et al., 1985).

The importance of RP gene expression is underscored by two human pathologies, which impair ribosome biogenesis, *5q*⁻ syndrome and Diamond Blackfan Anemia (DBA) (Teng et al., 2013). Both pathologies are characterized by macrocytic anemia, erythroid hypoplasia and an increased risk of AML. However, whereas *5q*⁻ syndrome is caused by a sporadic monoallelic deletion in the long arm of chromosome 5, including the gene for RPS14 (Pellagatti and Boultwood, 2015; Teng et al., 2013), DBA is a congenital disease caused by mutations in a number of RP genes (Teng et al., 2013). Although it was assumed in each

case that the disease was due to reduced protein synthetic capacity, depletion of RPs of either ribosomal subunit, leads to p53 stabilization and cell cycle arrest (Fumagalli et al., 2009). Subsequent studies in mouse models revealed that it is the apparent stabilization of p53, facilitated by the IRBC, which leads to the severe anemia (Barlow et al., 2010; McGowan et al., 2011). The IRBC is mediated by an RPL5/RPL11/5S rRNA ribosomal precursor complex, which upon impaired biogenesis of either subunit is redirected from assembly into 60S ribosomes to the binding and inhibition of the p53-E_3-ligase Hdm2 (Bursac et al., 2012; Donati et al., 2013). Interestingly, impairing either 40S or 60S biogenesis, does not alter the synthesis of the other subunit (Fumagalli et al., 2012), suggesting alternative functions of 40S and 60S ribosomes, as the excess ribosomal subunits cannot participate in protein synthesis (Fumagalli et al., 2012).

All RP genes belong to the 5′TOP family, which is thought to comprises less than 200 genes, but can account for up to twenty percent of the total mRNA in the cell (Gentilella and Thomas, 2012). Initially, we showed that the Target of Rapamycin (mTOR) controls their translation through the 5′TOP (Jefferies et al., 1997; Jefferies et al., 1994), with subsequent studies revealing that the translational response is mediated by mTOR complex 1 (mTORC1) phosphorylation of the initiation factor 4E binding proteins (4E-BPs), disrupting their binding and inhibition of 4E (Hsieh et al., 2012; Thoreen et al., 2012). However, recent reports suggest that the regulation of nascent 5′TOP translation may be more complex, also involving LARP1, an mRNA binding protein (Fonseca et al., 2015; Tcherkezian et al., 2014), although the underlying mechanism is as yet unresolved (Fonseca et al., 2015; Tcherkezian et al., 2014). LARP1 was first demonstrated to bind to the Poly(A) tails of mRNAs, and selectively control the levels of 5′TOP mRNAs (Aoki et al., 2013). These observations raised the possibility that LARP1, through regulating either the stability or translation of 5′TOP mRNAs, may be critical in mediating p53 responses to impaired ribosome biogenesis.

Here we found that depletion of LARP1, led to a strong reduction in RPL5 and RPL11 mRNAs, but, unexpectedly, resulted in p53 stabilization in an IRBC dependent manner. Moreover, despite the strong reduction in RPL5 and RPL11 mRNA transcript levels, the synthesis of their cognate proteins was unaffected. Consistent with this finding, the amount of RPL11 mRNA on large polysomes did not change in LARP1 depleted cells. However, there was a large decrease in the amount RPL11 mRNA sedimenting with small/non-polysomes, compatible with the reduction in its transcript levels. These observations led us to the finding that LARP1 mediated 5′TOP mRNA stability requires the 40S ribosome. In parallel, reassessing the genetic analyses of CD34+ bone marrow precursor cells from $5q^-$ patients (Wang et al., 2008), we found that LARP1 is also localized within the disease locus (Wang et al., 2008). Consistent with this observation LARP1 mRNA expression is reduced in $5q^-$ patients, suggesting that the previously noted general loss of RP mRNAs was not a secondary consequence of disrupting ribosome biogenesis (Pellagatti et al., 2008; Sridhar et al., 2009), but potentially a direct effect of depleting the LARP1-40S complexes. To determine whether LARP1 alone could play a role in the pathophysiology of $5q^-$ syndrome, we depleted its mRNA levels in human CD34+ bone marrow precursor cells, induced to differentiate along the hematopoietic lineage. This led to a reduction in 5′TOP mRNA levels, the induction of p53 and an anemic phenotype. Thus in higher eukaryotes, 40S

ribosomes control 5′TOP mRNA stability, which is mediated by LARP1, independent of the 40S ribosomes role in translation, with disruption of the LARP1-40S complex recapitulating the pathophysiological responses associated with *5q*⁻ syndrome.

Results

Depletion of LARP1 induces p53

LARP1 selectively sustains the levels of a number of RP mRNAs (Aoki et al., 2013). Given the essential role of newly synthesized RPL5 and RPL11 in the IRBC complex, we asked whether LARP1 depletion in HCT116 human colorectal carcinoma cells, affected the levels of RPL11 and RPL5 mRNAs. Northern blot analysis, of equally loaded rRNA samples, showed a large reduction in the levels of both transcripts upon treatment with a siRNA against LARP1 (siLARP1), versus a non-silencing (NS) control siRNA (siNS) (Figure 1A). We then reasoned that depletion of LARP1 would prevent p53 stabilization induced by impaired ribosome biogenesis. Unexpectedly, we found that LARP1 depletion alone led to p53 induction (Figure 1B). However, the extent of p53 induction was not of the magnitude observed by depleting either RPS6 or RPL7a, essential 40S and 60S RPs, respectively (Figure 1B). Similar results were obtained with human lung carcinoma cell line A549 (Figure S1A). Consistent with p53 induction, LARP1 depletion in HCT116 cells, led to apparent G1 arrest (Figure 1C), as observed with RPS6 or RPL7a depletion (Fumagalli et al., 2009; Fumagalli et al., 2012). To test whether these effects were mediated by the IRBC, we co-depleted LARP1 and RPL11 mRNAs. The results show that p53 induction by LARP1 depletion, in either HCT116 or A549 cells, is reversed by co-depletion of RPL11 mRNA, with the depletion of RPL11 mRNA alone having no effect on this response (Figures 1D and S1B). That the effects of LARP1 depletion on p53 are reversed by co-depletion RPL11 mRNA, suggests that loss of LARP1 triggers the IRBC. However, if these effects are mediated by the IRBC, the decrease in RPL5 and RPL11 transcripts was not of sufficient magnitude to prevent the production of the nascent RPL5/RPL11/5S rRNA complex (Donati et al., 2013).

Depletion of LARP1 does not affect RPL5 or RPL11 synthesis

The findings above suggested that LARP1 depletion would have only a partial inhibitory effect on RPL5 and RPL11 synthesis. Analysis of pulse-labeled newly synthesized proteins in NS or LARP1 siRNA treated cells with the methionine analogue L-azidohomoalanine (AHA), showed that total protein or newly synthesized biotinylated proteins by either amido black staining or streptavidin-IRDye800 detection respectively, were qualitatively equivalent (Figure 2A). However, LARP1 depletion led to the induction of both p53 and its target gene Hdm2, with no detectable change in RPL5 and RPL11 levels, consistent with the abundance of RPs present in mature ribosomes (Figure 2B). Similarly there was no change in RPS19, which we used as 40S RP control (Figure 2B). Compatible with the p53 stabilization induced by LARP1 depletion, the amount of newly synthesized p53 pulled down by the streptavidin beads increased as compared to control cells, as did Hdm2 (Figure 2B). However, despite the strong reduction in the levels of RPL5 and RPL11 mRNA following LARP1 depletion (Figure 1A), there was no visible effect on newly synthesized RPL5, RPL11 or RPS19 (Figure 2B). This was not due to non-specific binding, as no signal was

detected in extracts from AHA unlabeled cells (Figure S2A). Importantly, LARP1 overexpression, despite inducing an increase in 5′TOP mRNA levels (Figure S2B), did not affect newly synthesized RPs nor p53 levels (Figure 2C). Together the results suggested that loss of LARP1 leads to p53 induction independently of its effects on RP production.

Depletion of LARP1 has little impact on ribosome biogenesis

To determine the effect of loss of LARP1 on ribosome biogenesis, we measured steady-state levels of 18S and 28S rRNA by ethidium bromide (EB) staining, and nascent rRNA levels by pulse labeling with ^{3}H-uridine (Donati et al., 2013; Fumagalli et al., 2009). As a control, we depleted RPS6, which disrupts 18S rRNA biogenesis without affecting that of 28S rRNA (Fumagalli et al., 2009; Volarevic et al., 2000). An EB-stained agarose gel shows that LARP1 depletion, as compared to controls, had no impact on total 18S or 28S rRNA levels, whereas depletion of RPS6 led to a clear decrease in total 18S rRNA levels (Figure 2D). However, unlike RPS6 depletion, which almost totally abolished nascent 18S rRNA maturation, LARP1 depletion had only a small effect on the rate of incorporation of ^{3}H-Uridine into newly synthesized 18S and 28S rRNA, as compared to controls (Figure 2D). The small increase in p53 levels upon LARP1 knockdown is consistent with the small effect on of LARP1 depletion on ribosome biogenesis (Figure 2D). These effects are paralleled by an ~20% decrease in ^{3}H-Leucine incorporation into nascent protein in LARP1-depleted cells (Figure 2E). It has been reported that depletion of RP mRNAs leads to the induction of eukaryotic elongation factor 2 (eEF2) phosphorylation and inhibition of global translation, but does not alter the levels of newly synthesized 5′TOP proteins (Gismondi et al., 2014). We also find that LARP1 depletion leads to an increase eEF2 phosphorylation, though to a lesser extent than 2-deoxy glucose (2-DG), a potent inducer of this response (Figure S2C). Thus the small impact of LARP1 depletion on ribosome biogenesis and protein synthesis, is consistent with the limited rise in p53.

LARP1 differentially affects the distribution of RP mRNAs on polysomes, but not their translational usage

Recent studies have ascribed either a positive (Tcherkezian et al., 2014) or a negative role (Fonseca et al., 2015) for LARP1 in selective translation of 5′TOP mRNAs. However, that LARP1 depletion had little to no effect on the generation of newly synthesized RPs (Figure 2B), prompted us to determine the effect of its loss on the distribution of RPL11 on polysome gradients. Although the distribution of absolute amount of RPL11 mRNA, measured by quantitative real time PCR (RT-qPCR) or northern blot analysis does not change significantly in large polysomes of LARP1 depleted cells, as compared to controls (Figure 3A and S3A), the amount present in the small/non-polysomal area of the gradient is significantly reduced (Figure 3A and S3A). This observation is not unique for RPL11 mRNA, as it was recapitulated by RPL5 and RPL23 mRNAs (Figures 3B and 3C), whereas we see little difference in the distribution of a non-5′TOP mRNA, such as heat shock protein A1A (Figure 3D). The levels of individual mRNAs were determined in total input RNA (Figure S3B). The reduction in RP mRNAs sedimenting in the small/non-polysomal area is paralleled by a slight decrease in small/non-polysomes (Figure 3A), consistent with the small reduction in newly synthesized proteins (Figure 2E). Given these apparent global effects on translation, with no effect on newly synthesized RPs (Figure 2B), we asked

whether their stability could be involved in maintaining their overall levels. To test this, we pulse-labeled cells with ^{35}S methionine/cysteine, then chased with an excess of non-radioactive methionine/cysteine. At the times indicated during the chase, we harvested the cells and immunoprecipitated RPL5 or α-tubulin (Figure 3E). In LARP1 depleted cells, as compared to controls, higher levels of immunoprecipitated ^{35}S methionine/cysteine labeled RPL5 are detected as early as 30 mins after initiating the chase, which is more evident at 5 and 10 h, with no differences observed for α-tubulin (Figure 3E). Taken together the results show that in LARP1 depleted cells there is a decrease in the levels of RP mRNAs on small/non-polysomes, whereas their levels are preserved on large polysomes, allowing the continued synthesis of their cognate proteins.

The 5′TOP is required for LARP1 interaction

The results above support a major role of LARP1 in mediating 5′TOP mRNA stability. Aoki et al. have shown that LARP1, not only selectively sustains the levels of 5′TOP mRNAs, but also binds the 3′ terminus Poly(A) tail (Aoki et al., 2013). To determine if the 5′TOP is required for selective maintenance of mRNA stability by LARP1, we generated Tet-ON stable cell lines expressing either a wild type (WT) or mutant (MU) 5′TOP reporter, containing either a WT 5′TOP construct of RPL32 fused with the β-globin gene or a mutant (MU) 5′UTR, where we placed purines in the location of 5′TOP (see Experimental Procedures). The WT construct behaves like RPL11 in growing cells, distributed equally among the non-polysome and polysome fractions, with rapamycin treatment causing a redistribution to the non-polysomal fraction (Figure 4A). In contrast, the MU-reporter, expressing comparable amount of β-globin (Figure S4A), is found almost exclusively in polysomes in the absence or presence of rapamycin (Figure 4A). To determine if LARP1 interacts more specifically with the WT-reporter compared to the MU-reporter, extracts from doxycycline-induced cells were immunoprecipitated with either a LARP1 or IgG control antibody. The results show that ~15-fold more of the WT-RPL32 construct is co-immunoprecipitated with the LARP1 antibody versus the IgG control (Figure 4B). In contrast, less than a 2-fold increase over the IgG control is observed for the MU-RPL32 reporter (Figure 4B). To analyze the effect of LARP1 on the half-life of the WT- and MU-RPL32 reporters, both cell lines were induced with doxycycline, then transfected with either the LARP1 or control siRNA, deprived of doxycycline and the fate of newly transcribed reporters followed over time. The results show that when normalized to 18S rRNA or 28S rRNA, LARP1 depletion induces a decrease in the half-life of the WT-RPL32 transcript versus the control (Figure 4C). In contrast, the MU-RPL32 reporter, which has a shorter half-life, is unaffected by LARP1 depletion (Figure 4C). Consistent with this finding overexpression of exogenous WT-RPL32 reporter, but not MU-RPL32 reporter, reduced the amount of endogenous 5′TOPs (Figure 4D). The findings show that the ability of LARP1 to interact and stabilize 5′TOP mRNAs is dependent on the 5′TOP sequence.

40S ribosomes are required for 5′TOP mRNA stability

As LARP1 depletion led to a selective loss RP mRNAs migrating with small/non-polysomes, particularly near the area of free 40S ribosomes, we asked whether depletion of a 40S versus a 60S RP had a differential effect on the levels of other RP mRNAs. To test this possibility, we depleted essential RPs of either subunit and measured their effects on

stability of RPL5 and RPL11, as well as eukaryotic elongation factor (eEF)-1α, a non-RP 5′TOP mRNA. Compared to control cells, siRNA depletion of either 40S RPS6 or RPS23 led to decreased levels of all three 5′TOP mRNAs (Figure 5A). Unexpectedly depletion of 60SRPs, RPL7a or RPL23, induced the opposite response (Figure 5A). These effects are p53-independent, as depletion of RPL5 or RPL11 induces the same increase in the levels of 5′TOP mRNAs, as the other 60S RPs (Figure 5A). Moreover, co-depletion of a 40S and 60S RP, shows that the effect of 40S RP depletion is dominant with respect to the levels of 5′TOP mRNAs, whereas co-depletion of two RPs from the same subunit does not enhance either response (Figure 5A). These responses are not recapitulated for a non-5′TOP mRNA, such as β-actin mRNA (Figure 5A). To further test the importance of the 40S ribosome, we first depleted RPS6 and then transfected the mouse RPS6 cDNA, and under these conditions we restored 5′TOP levels to that of NS treated control cells (Figure S5A). This response was not unique to 40S RP-depletion, as similar results were obtained by depletion of U3 small nucleolar RNA-associated protein (hUTP18) (Figure S5B), an essential component of the mammalian small subunit (SSU) processome, required for 40S ribosome maturation (Holzel et al., 2010). Thus depletion of 40S ribosomes, leads to a decrease in 5′TOP mRNA, but not non-5′TOP mRNA levels, consistent with a critical role in maintaining 5′TOP mRNAs.

To determine whether changes above are dependent on an intact 5′TOP sequence, as for LARP1 (Figure 4C), we used the WT-RPL32 and MU-RPL32 reporter cell lines (Figure 4A). We first induced both cell lines with doxycycline and then treated cells with RPS6 or RPL7a siRNAs. RPS6 depletion led to a decrease in the WT-RPL32 reporter levels, whereas they were enhanced by RPL7a depletion, with no differences observed for the MU-RPL32 reporter (Figure S5C). Consistent with these findings, LARP1 immunoprecipitates from RPS6-depleted cells have less RPL23 and RPL11 mRNA bound, compared to control cells, whereas those depleted of RPL7a had more RPL23 and RPL11 mRNA bound than controls (Figure 5B). In contrast, under all three conditions there was no difference in LARP1's interaction with the non-5′TOP mRNA βactin (Figure 5B). To determine the effect on reporter half-life, we conducted the equivalent experiment as we had for LARP1 depletion above (Figure 4C). In both cases the extent of RPS6 depletion, normalized to 28S rRNA, or RPL7a, normalized to 18S rRNA, was equivalent (Figure S5D). RPS6 depletion led to a decrease in the half-life of the WT-RPL32 reporter, normalized to 28S rRNA, whereas RPL7a depletion led to an increase in the half-life of the WT-RPL32 reporter, when normalized to 18S rRNA, with no such differences observed on the MU-RPL32 reporter (Figure 5C). It should be noted that when the levels of WT-RPL32 reporter from cells are normalized to either 18S or 28S rRNA the results are equivalent (Figure S5E), as they were in the case of LARP1 depletion (Figure 4C). Taken together the results show that 40S ribosomes are also required for the stability of 5′TOP mRNAs.

Native 40S ribosomes control 5′TOP mRNA stability

Impairing one ribosomal subunit biogenesis by depleting an essential RP, does not alter the synthesis of the other subunit, which accumulates as a free 40S or 60S ribosome in the non-polysomal fraction of the gradient (Fumagalli et al., 2009). Given that increased 5′TOP mRNA stability is dependent on 40S subunit availability (Figures 5A and 5B), we tested whether when free 40S are reduced by RPS6 depletion or increased by RPL7a depletion,

they affect the distribution of RPL11 mRNA on polysomes. The depletion of either RP leads to a similar decrease in the mean polysome size and in the distribution of RPL11 mRNA, as compared to controls (Figures 6A and 6B). However, RPS6 depletion induces a decrease in free 40S ribosomes that is paralleled by a decrease in co-sedimenting RPL11 mRNA (Figure 6A). In contrast, free 40S ribosomes and RPL11 mRNA were strongly elevated in cells depleted of RPL7A (Figure 6B). Moreover, in LARP1 depleted cells, the RPL11 mRNA migrating with free 40S subunits is lost (Figure 6C), suggesting that the association of 5′TOP mRNAs with free 40S subunits is LARP1-dependent. Consistent with this, LARP1 protein co-migrating with free 40S subunits in control cells, is almost completely absent in RPS6 depleted cells, whereas it is highly elevated in RPL7a depleted cells (Figure 6D). RPL11 mRNA levels, measured in total cellular RNA extracts was compatible with the polysome data (Fig S6A). The results suggest that LARP1 and free 40S ribosomes form a complex with 5′TOP mRNAs.

To determine whether this is the case, whole cell extracts from control cells were incubated with the protein crosslinking agent dithiobis-succinimidyl propionate (DSP), the 40S fraction collected on polysome gradients and then subjected to immunoprecipitation with a LARP1 antibody or an IgG control antibody (Figure S6B). The results show that 18S rRNA, 40S RPS6 and RPS19 (Figure 6E), as well as 5′TOP mRNAs, analyzed by RNAseq (Figure 6F), are highly enriched in the LARP1 immunoprecipitates, as compared to the IgG controls. In the case of the 5′TOP mRNAs, the RP mRNAs appear to represent a subfamily, which is even more enriched than the other 5′TOP mRNAs (Figure 6F and Table S1), whereas, abundant non-5′TOP mRNAs are not enriched in the LARP1 versus IgG immunopreciptates (Figure 6F). Given that the levels of 5′TOP mRNAs (Figure 6B) and LARP1 (Figure 6D) co-migrating with free 40S ribosomes increase in RPL7a depleted cells we asked whether their direct association was enhanced. The results show that as compared to control cells, in RPL7a depleted cells the levels of free 40S subunits are increased as are those of LARP1 (Figures S6C and S6D, respectively). This increase was associated with a further enrichment of 18S rRNA and 5′TOP mRNAs in the LARP1 immunoprecipitates, as compared to the control (Figure 6G). In contrast to RPL7a depletion, rapamycin treatment does not affect free 40S ribosomes levels, but leads to the accumulation of 5′TOP mRNAs in the small/non-polysome area of the gradient (Figure 4A). In parallel, we find that rapamycin enhances the levels of LARP1 migrating with free 40S ribosomes (Figure 6H). Immunoprecipitates of DSP-treated rapamycin whole cell extracts, which has no effect on the free 40S subunit distribution (Figure S6E), shows that the amounts of 18S rRNA and 5′TOP mRNAs increase in the LARP1 immunoprecipitates, without changing the amounts of non-5′TOP mRNAs such as βactin (Figure 6I). Thus LARP1 forms a complex with 40S ribosomes and 5′TOP mRNAs, whose levels are enhanced by the availability of free 40S ribosomes or rapamycin treatment.

Pathological implications of reduced levels of LARP1 in *5q*⁻ syndrome

Previous studies showed that *5q*⁻ patients have reduced levels of RP mRNAs, as well as those of a number of protein synthesis initiation and elongation factors (Pellagatti and Boultwood, 2015; Sridhar et al., 2009), which we confirmed by comparing a large cohort of $CD34^+$ precursor cells from *5q*⁻ syndrome patients, with those of healthy individuals or

other non-*5q*⁻ myelodysplastic (MDS) patients (Figure 7A). These effects were suggested to be a consequence of impaired ribosome biogenesis caused by the loss of RPS14, one of ~ 40 genes residing in the common deleted region (CDR) of *5q-* patients (Pellagatti et al., 2008). However, given that loss of LARP1 leads to a reduction in 5′TOP mRNA stability and the induction of p53, and that the LARP1 gene is located at 5q33.2, in close proximity to the CDR, raised the possibility that its loss is associated with *5q*⁻ syndrome. A case by case reassessment of the published genetic analyses of CD34+ bone marrow precursor cells from *5q*⁻ patients (Wang et al., 2008), showed the that LARP1 gene is included within the *5q*⁻ CDR, consistent with reduced LARP1 mRNA levels in $CD34^+$ bone marrow precursor cells of patients with *5q*⁻ syndrome, when compared to those of healthy individuals or of non-*5q*⁻ MDS patients (Figure 7B). To determine the physiological impact of the loss of LARP1 alone, we depleted its mRNA levels to ~ 50% in human peripheral adult CD34+ cells induced to differentiate along the erythrocytic lineage (Figure 7C). Critically, depletion of only LARP1 led to a reduction in 5′TOP mRNA levels and enhanced expression of p53 target genes (Figure 7C), previously shown to be the cause of *5q*⁻ syndrome (Barlow et al., 2010). Consistent with anemic phenotype displayed by *5q*⁻ syndrome patients, the reduction in LARP1 led to a ~ 20–30% decrease in the induction of both α and β globin mRNAs, which was further reduced at later time points in erythroid differentiation (Figure 7D). As only one allele of RPS14 and LARP1 are lost in *5q*⁻ syndrome, this raised the question of whether loss of both genes would have a more profound effect on the induction of p53. We tested this possibility by siRNA depletion of RPS14, or RPS6 as a control, alone or in combination with LARP1 in HCT116 cells. The results show that the depletion of RPS14, like RPS6, led to the induction of p53 (Figure 7E), though the effects are less profound for RPS14, similar to earlier findings (Dutt et al., 2010). In both cases the amplitude the p53 response is strikingly enhanced by co-depletion of LARP1 (Figure 7E). These observations suggest that in *5q*⁻ patients, the reduction of LARP1 along with RPS14, further impacts on the pathophysiology of the disease with respect to loss of RPS14 alone (see model, Figure 7F).

Discussion

We initially set-out to understand the importance of LARP1 in regulating the IRBC following impaired ribosome biogenesis, given recent studies underscoring its role in regulating the levels of 5′TOP mRNAs (Aoki et al., 2013) and their translation (Fonseca et al., 2015; Tcherkezian et al., 2014). The sharp reduction in both RPL5 and RPL11 transcript levels following acute depletion of LARP1, are consistent with the findings of Aoki et al, who observed that similar treatment caused a selective decrease in the levels of a number of 5′TOP mRNAs, without affecting a large number of representative non-5′TOP mRNAs (Aoki et al., 2013). Here we demonstrate that the decrease in 5′TOP mRNA levels following LARP1 depletion, or that of 40S ribosomes, is mediated through a decrease in their half-lives. The loss of 5′TOP mRNA stability induced by LARP1 depletion was paralleled by a small induction of p53 and the accumulation of cells in G1 phase. That the p53 response was suppressed by co-depletion of RPL11 and disruption of the IRBC, was consistent with the small inhibitory effect on ribosome biogenesis caused by loss of LARP1. Although, the inhibitory effect did not appear to be due to a reduction in RPs, we cannot exclude a

stoichiometric imbalance amongst RPs during ribosome biogenesis, such that one became limiting during the process. It is also possible that the inhibition of ribosome biogenesis, leading to the induction of p53, is caused by a reduction in a 5′TOP mRNA (s), whose cognate protein is involved in processing of nascent ribosomes, such as nucleolin.

The failure to observe a decrease in newly synthesized RPs in the face of a sharp drop in their respective RP mRNAs, raised the possibility of the selective translational upregulation of RP mRNAs following LARP1 depletion (Fonseca et al., 2015; Fumagalli et al., 2009). Initially, by plotting the data as a percentage of the total, this appeared to be the case (data not shown). However, when we determined the amount of RPL11 transcripts in each fraction, we found that mRNA associated with the polysome fraction was preserved, whereas that in the small/non-polysome fraction was reduced. Plotting the data as a percentage of the total, as we did earlier and others have done recently (Fonseca et al., 2015; Fumagalli et al., 2009), or not considering the small/non-polysome fractions (Tcherkezian et al., 2014), can be misleading. The data indicated that the RP mRNAs associated with polysomes were responsible for maintaining the levels of RPs, suggesting growing cells can cope with the production of 5′TOP cognate proteins even in absence of this 5′TOP mRNAs reservoir associated with the 40S ribosomes. This raised the possibility that, to maintain RP levels, there had to be an increase in either RP mRNA transit times or in RP half-life. The increase in eEF2 phosphorylation argued against enhanced rates of translation, whereas the pulse chase experiments with RPL5 favored an increase in protein half-life. It will be of interest to determine the underlying mechanism that controls RP half-life, which appears can buffer ribosome biogenesis.

The finding that depletion of a 40S RP or 60S RP mRNA differentially affects 5′TOP stability, led us to the unexpected role of 40S ribosomes in the autogenous control of 5′TOP mRNA stability. Pierandrei-Amaldi et al, first suggested that the stability of RP mRNAs maybe regulated autogenously by RPs (Pierandrei-Amaldi et al., 1985). This prediction was based on studies with anucleolated *Xenopus laevis* embryos, which lack the rRNA gene cluster, but can survive up to stage 30 of embryogenesis on maternal ribosomes (Pierandrei-Amaldi et al., 1985). In WT and mutant embryos at stage 30, the RP mRNAs are mobilized on to polysomes to further increase ribosome content. However, in the anucleolated embryos, the newly synthesized RPs and RP mRNAs are rapidly degraded, and there are no free 40S ribosomes, as all are recruited into polysomes, in an apparent attempt to survive (Pierandrei-Amaldi et al., 1985). We speculate that the reduction of free 40S ribosomes leads to RP mRNA instability, explaining the autogenous mechanism described in anucleolated embryos.

The characterization of the 5′TOP mRNAs initially stemmed from studies showing that under conditions of repressed cell growth the translation of RP mRNAs was selectively inhibited (Avni et al., 1994), which we later showed was the case for rapamycin treatment (Jefferies et al., 1997; Jefferies et al., 1994). A subsequent comprehensive analysis of human transcripts, based on the DBTSS (Yamashita et al., 2008), identified over 1600 5′TOP mRNAs, however, applying translational control as a criteria, limited the number to only 96 genes (Meyuhas and Kahan, 2015). Here, in an unbiased analysis using the DBTSS, we find in the LARP1-40S complexes from growing cells, that there is an enrichment of 368

mRNAs of which 310, or 84%, are 5′TOP mRNAs. Notably, of the first 120 genes listed, 115, or 96%, are 5′TOP mRNAs (Table S1). Given the large number 5′TOP mRNAs enriched in the LARP1-40S complex, it may be that the role of 5′TOP sequence in translation is secondary to its role in mRNA stability. Of the small subset of enriched non-5′TOP mRNAs, many appear to contain a degenerative 5′TOP sequence, such that their identities will need to be confirmed by targeted mapping of the TSS. Moreover, amongst the enriched 5′TOP mRNAs, a portion appear to be associated with cellular processes distinct from ribosome biogenesis and the RP mRNAs potentially represent a hierarchical subfamily. Thus it will be of interest to determine if there is a relationship between these two families and evolutionarily, which elements give the RP mRNAs their apparent uniqueness. Furthermore, it should be clarified whether these elements reside only within the oligo pyrimidine tract, or elsewhere in the 5′ untranslated region.

The question which emerges from these observations is the identity of the LARP1-40S ribosome complex. We find that from the 40S fraction nearly all the LARP1 protein is removed by immunoprecipitation, 30–40% of the 5′TOP mRNAs, but only ~1% of the 18S rRNA (data not shown). Given that many distinct mRNAs are sedimenting in this fraction, raises the possibility of other unique 40S complexes. In the case of the LARP1-40S ribosome complex, LARP1 is known to interact with poly(A)-binding protein (PABP) in the presence or absence of mRNA (Aoki et al., 2013), although the domain of interaction is not clearly defined (Fonseca et al., 2015; Tcherkezian et al., 2014). That LARP1 recognizes the 5′TOP motif (Fonseca et al., 2015) and that the PABP can interact directly with both LARP1 (Aoki et al., 2013) and eIF4G1 (Sonenberg and Hinnebusch, 2009), point to a potential role of a 48S-like preinitiation complex in controlling 5′TOP mRNA stability. Defining the molecular constituents of the LARP1-40S ribosome complex will be a key step in understanding its extra ribosomal role in 5′TOP mRNA stability. In this regard it, is important to note that mTORC1 not only regulates the translation of 5′TOP mRNAs (Gentilella and Thomas, 2012), but apparently their stability (Fonseca et al., 2015), suggesting a potential crosstalk between the LARP1-40S ribosome complex and signaling components of the mTORC1 pathway. Whether unique populations of 40S ribosomes are engaged in distinct ribosomal complexes and the role of mTORC1 in integrating the translation and stability of 5′TOP mRNAs needs to be addressed.

5q^{-} syndrome serves as an appropriate pathological context to query the importance of the maintenance of 5′TOP mRNA stability. RPS14 plays a major role in the onset of bone marrow failure (Barlow et al., 2010; Schneider et al., 2016), however we show in CD34+ cells induced to differentiate along the hematopoietic lineage, that depletion of LARP1 mRNA alone, recapitulates not only the activation of p53 and an anemic phenotype, but the decrease in 5′TOP mRNA levels seen in *5q*$^{-}$ patients. It is thought that ribosome biogenesis is reduced in CD34+ cells, but that upon differentiation to proerythroblasts, it is dramatically enhanced to generate the large amounts of α and β globin required for mature red blood cells (Flygare and Karlsson, 2007). Importantly, it has been shown that protein synthesis and mTORC1 activities are low in CD34+ cells (Signer et al., 2014), which could increase the amount of LARP1-40S complexes, acting to stabilize 5′TOP mRNAs. By depleting LARP1 in CD34+ cells from healthy donors we show that a loss of 5′TOP mRNAs in *5q*$^{-}$ syndrome patients is not a secondary consequence of reduced translation, but instead a direct cause of

the loss of LARP1 and RPS14. Moreover, it is p53 stabilization which leads to the macrocytic anemia (Teng et al., 2013) and this response is strikingly enhanced by the combined loss of LARP1 and RPS14, which would appear to be particularly relevant in the pathophysiology of *5q*$^{-}$ syndrome, where both native 40S ribosomes and LARP1 are reduced.

STAR METHODS

Cell Culture

HCT116 human colorectal carcinoma cell lines was obtained from the American Type Culture Collection and maintained in DMEM supplemented with 10% heat-inactivated fetal bovine serum (Sigma-Aldrich, St Louis, MO, USA). Double stable inducible HCT116 rtTA/TetO-WT-L32TOP-β-Globin-MS2(12X) or HCT116 rtTA/TetO-MU-L32TOP-β-Globin-MS2(12X) were obtained by generating rtTA expressing cells by neomycin selection, followed by a second round of transfection with the plasmids TetO-WT-L32TOP-β-Globin-MS2(12X) or TetO-MU-L32TOP-β-Globin-MS2(12X) by puromycin selection. Clones were screened based on doxycyline inducibility and β-Globin reporter expression levels, in both cell lines.

Reagents and plasmids

RNAimax transfection reagent, TRIZOL RNA extraction reagent, Click-iT Protein Reaction Buffer kit, Click-iT AHA (L-azidohomoalanine) and the Biotin-Alkyne conjugate were purchased from Invitrogen (Carlsbad, CA, USA). The Pierce Neutravidin-Agarose beads were purchased from Thermo Scientific and the Streptavidin-IRDye 800CW were purchased from Li-Cor Biotechnology (Lincoln, NE). EN^{3}HANCE autoradiography enhancer, ^{3}H-Uridine and ^{3}H-L-leucine were purchased from Perkin-Elmer. The SYBR green qPCR kit was from Roche (Basel, Switzerland). The Bradford Reagent was from Bio-Rad. The polyclonal anti-LARP1 and anti-L5 antibodies were from Bethyl, and the monoclonal anti-L11 from Invitrogen. The polyclonal anti-p53 was purchased from Santa-Cruz Biotechnology and the anti-α-tubulin (clone B-5-1-2) was purchased from Sigma-Aldrich. MagnaCHIP Protein A/G magnetic beads mix was from Millipore. Goat anti-(mouse IgG)-peroxidase conjugate and goat anti-(rabbit IgG)-peroxidase conjugate were from Dako. The Placental Rnase inhibitor was purchased from NEB (New England Biolabs). TetO-WT-L32TOP-β-Globin-MS2(12X)-Puro was generated by modifying the RPL32-β-Globin plasmid from Damgaard et al. (Damgaard and Lykke-Andersen, 2011). Briefly twelve repeats of the MS2-binding site were inserted downstream of β-Globin gene using an ApaI restriction site. TetO-MU-L32TOP-β-Globin-MS2(12X)-Puro was generated by site-directed mutagenesis as previously described (Gentilella et al., 2008) using specific primers (see Table S2). LARP1 over expression plasmid was described elsewhere (Fonseca et al., 2015) and was kindly provided by Bruno Fonseca. The Murine RPS6-pAdLOX expression plasmid was a generous gift from Mario Pende. The sequences of siRNAs used in the experiments, siRPS6, siRPL7a, siRPL23, siRPS23, siLARP1#1, siLARP1#2, siNS, siRPL11, siRPL5, siRPS14 and siUTP18 are reported in Table S2. For each treatment the amount of siRNA transfected was maintained constant between samples, by using siNS where required.

Protein analysis

Cell protein extracts for western blot analysis were prepared by using a 1% SDS lysis buffer (Tris pH7.4 50mM, SDS 1%) supplemented with the protease inhibitor cocktail (SIGMA), phosphatase inhibitor cocktail 3 (SIGMA), sodium orthovanadate 2mM and 100 U/ml of benzonase. After lysis, cell lysates were incubated 30′ on ice followed by centrifugation at 13,000 rpm for 10′. Protein concentrations were determined for supernatants by the BCA assay (Pierce). 25 μg of total protein extracts were resuspended in Laemmli SDS-sample buffer and after treatment at 95C for 5min, proteins were separated on 10% SDS–polyacrylamide gels by electrophoresis, and transferred to PVDF membranes. Blots were stained with amido black to confirm equal loading and transfer of proteins and then reacted with the western blots probed with the indicated antibodies. Immunoblots were developed using secondary horseradish peroxidase-coupled antibodies and an enhanced chemiluminescence kit (GE Healthcare).

RNA analysis

Total cellular RNA was isolated using TRIzol reagent (Invitrogen) according to the manufacturer's instructions. Total RNA (5 to 10 μg) was resolved on formaldehyde-containing 1.2% agarose gel and transferred to Hybond-N+ nylon membranes (GE Healthcare) and crosslinked by ultraviolet irradiation. The filter was prehybridized 1 hr at 55°C in Church phosphate buffer (7% SDS, 1mM EDTA) and hybridized for 20 h at 55°C with a biotynylated oligo complementary to RPL11, RPL5, eEF1α, β-Globin or GAPDH mRNAs (10 ng/ml). The blot was then rinsed three times for 5 min with 2X SSC 0.1% SDS at 55°C, then hybridized with streptavidin-HRP at 28°C for 30 min. The membrane was washed four times with PBS 1X, 0.5% SDS at 28°C for 5 min. The filter was subjected to enhanced chemiluminescence reaction (GE Healthcare) and exposed to Fuji XAR-5 film with Kodak intensifying screen for 30 min. To verify equivalent RNA loading on northern blot membrane, the filter was re-hybridized with a β-Actin probe. (see Table S2).

Real-time PCR

Total cellular RNA was isolated using TRIzol reagent (Invitrogen) according to the manufacturer's instructions. cDNA synthesis and quantitative real-time PCR were performed as described previously (Gentilella and Khalili, 2011). The sequences of primers utilized to amplify RPL11, GAPDH, RPL23, RPS6, RPL7a, βActin, Firefly are reported in Table S2.

Polysome Profile analysis

Distribution of mRNAs across sucrose gradients was performed as described earlier (Fumagalli et al., 2012), except for minor modifications. Briefly, 10^6 HCT116 cells were plated in 100 mm dish and transfected with the indicated siRNA as described above. 24 or 48 h after transfection, cycloheximide (CHX) was added to the medium at 37°C for 5 min at a concentration of 100 μM. Cells were washed twice with cold PBS supplemented with CHX, scraped on ice and pelleted by centrifugation at 3000 rpm for 3′. Cell pellets were resuspended in 250 μl of hypotonic lysis buffer (1.5 mM KCl, 2.5 mM $MgCl_2$, 5mM Tris HCl pH7.4, 1mM DTT, 1% sodium deoxycholate, 1% Triton X-100, 100 μg/ml CHX) supplemented with mammalian protease inhibitors (SIGMA) and RNAse inhibitor (NEB) at

a concentration of 100 U/ml and left in ice for 5′. Cell lysates were cleared of debris and nuclei by centrifugation for 5′ at 13000 rpm. Protein concentrations were determined by BCA assay and 500 μg of lysate were loaded on 10–50% sucrose linear gradients containing 80 mM NaCl, 5 mM MgCl2, 20 mM Tris HCl pH7.4, 1 mM DTT, 10 U/ml Rnase inhibitor with a BIOCOMP gradient master. Gradients were centrifuged on a SW40 rotor for 2 hr at 32000 rpm or 3 hr at 35000 rpm as indicated in the figure legends. Gradients were analyzed on a BIOCOMP gradient station and collected in 12 fractions ranging from light to heavy sucrose. Fractions were supplemented with SDS at a final concentration of 1% and placed for 10 min at 65°C. To each fraction was added 1ng of firefly luciferase mRNA, followed by phenol-chloroform extraction and precipitation with isopropanol. Purified RNAs from each fraction were reverse-transcribed and subjected to qPCR. mRNA quantification was normalized to firefly mRNA.

RNA-immunoprecipitation Assays

HCT116 cells were plated in 100-mm dishes at 1.0×10^6 cells. Cells were transfected with the siRNA at a final concentration of 20nM using RNAimax reagent (Invitrogen), and 48 hr later cells were lysed with RIP buffer as described in Keene et al. (Keene et al., 2006). Cell lysates were centrifuged and cleared from debris, and anti LARP1- or normal rabbit serum IgG-loaded beads were added to 500 μg of total cell extract. Samples were incubated at room temperature for 2 hr. Beads were washed four times with NT2 buffer (50 mM Tris pH7.4, 150 mM NaCl, 5 mM MgCl2, 0.05% NP-40), then 20% of the immunoprecipitated complex was used for protein analysis and resuspended and probed for LARP1 protein as described above. 80% of the immunocomplexes isolated were first supplemented with 1ng of firefly luciferase mRNA, then processed for RT-qPCR as described above. Firefly luciferase served to normalize samples. Data are reported as percentage enrichment of anti-LARP1-immunoprecipitated mRNA over normal rabbit serum precipitated material. For LARP1 immunoprecipitation from 40S fraction the above protocol was modified as follows: HCT116 cells were pretreated with CHX as explained for polysome profile analysis. Cell pellets were lysed and resuspended in 225 μl of complete hypotonic lysis buffer added with 2.5 mM DSP crosslinker and left at RT for 5′. 25 ul of 1M Tris-HCl pH 7.4 was added and cell lysates were incubated at RT for additional 5′. Polysome separation was carried out as described above and after fractionation, the portion of the gradient corresponding to the 40S subunit was isolated and processed. 40S fractions from replicate gradient were pooled and centrifuged at 4C through an Amicon Ultra-4 membrane until the volume was concentrated 20 times (40S Input lysate). LARP1 RNA-IP was then carried out as described above.

Cell-cycle analysis

Cell-cycle analysis was performed using the propidium iodide cell-cycle reagent protocol as described previously (Gentilella et al., 2008). Briefly, HCT116 cells were grown overnight in DMEM supplemented with 10% serum, then transfected with 20 nM siRNA or nonspecific siRNA using RNAimax. After 48 hr, cells were harvested, fixed with 70% ethanol and treated for 30 min with propidium iodide solution at 37°C. Samples were analyzed using FACS Canto System. The data are representative of three different experiments.

De novo protein analysis

Cells were transfected with 20nM siLARP1 or control siNS sequence as described above for 48 hr. Before lysis, cells were placed in methionine-free DMEM supplemented with 25 μM Azyde-Homoalanine (AHA) for 2 hr. AHA-labeled proteins were chemically processed according to manufacturer's protocol and 200 μg of biotin-alkyne-conjugated proteins were resuspended in 500 μl of PBS, NaCl 150 mM, SDS 0.1% and protease inhibitors and incubated 4 hr at 4°C with streptavidin-agarose beads. Streptavidin-biotin conjugates were washed three times with 500ul of wash solution (Tris-HCl pH 7.4 50 mM, NaCl 150 mM, SDS 0.1%), resuspended in 2x Laemmli buffer, resolved on 10% SDS PAGE and probed with the indicated antibodies. ^{35}S-Met/Cys metabolic pulse-chase analysis was carried out as described previously (Gentilella and Khalili, 2011).

Lentiviral prep and CD34+ infection

Control shRNA and LARP1 shRNA lentiviral particles were generated as described previously (Fonseca et al., 2015). Adult human bone marrow was harvested under a protocol approved by the institutional review board (IRB), and CD34+ cells were purified using CD34+ MACS microbeads. CD34+ cells were transduced with Control shRNA or with a combination of two LARP1 shRNAs sequences lentiviral particles. Cells were cultured in Serum-Free Expansion Medium supplemented with 100 U/ml of penicillin/streptomycin, 2 mM glutamine, 40 μg/ml lipids (Sigma), 100 ng/ml stem cell factor, 10 ng/ml interleukin-3, 10 ng/ml interleukin-6 and 0.5 U/ml erythropoietin as previously described (Ebert et al., 2008). On day 7 cells were harvested and total RNA was purified.

Microarray analysis of 5q$^-$ patients

Microarray data from 47 *5q*$^-$ MDS patients, 136 non *5q*$^-$ MDS patients and 17 healthy controls included in the Gene Expression Omnibus (GEO) series with accession number GSE19429 (Pellagatti et al., 2010) was normalized using the Robust Multichip Average (RMA) algorithm from the *oligo* R package (Carvalho and Irizarry, 2010). Fold changes among groups of those probes corresponding to LARP1, a panel including RPs and other known 5′-TOP genes, as well as another panel of non-5′TOP genes as a control were analyzed. T-tests were used to unveil differential expressed genes between MDS patients versus healthy controls with a significance level of 0.05. Genes with a False Discovery Rate (FDR) under 5% were also identified.

RIP-seq data analysis

LARP1 IP, IgG IP and INPUT libraries from two biological replicates were sequenced on Illumina HiSeq 2500 platform in single end mode resulting in 50 base length reads at CRG Genomics Core Facility. Library depths oscillated between 35 to 51 million reads. After filtering out ribosomal RNA reads (representing around 85% of total), remaining ones were aligned against human transcriptome based on Ensembl annotation (genome release GRCh38) using TopHat version 2.1.1 (Trapnell et al., 2009). Alignments were processed with featureCounts function from Subread version 1.20.6 (Liao et al., 2013) discarding multi-mapped and multi-overlapped reads and counting unique-mapping ones against gene models. Genes showing less than one count per million either in INPUT or LARP1 IP were

filtered out and raw count values were normalized following the median ratio method (Anders et al., 2010). For each gene, the average of normalized counts among replicates was kept for each condition (LARP1 IP, IgG IP and INPUT) and background noise given by IgG IP was subtracted from LARP1 IP, keeping only genes which unspecific binding resulted lower than that in LARP1 pull down. An abundance threshold was defined, keeping only those genes showing an INPUT above the median in Transcripts per Million (TPM). Fold Enrichment over INPUT was computed according to the formula *Enrichment = (LARP1 IP - IgG IP)/INPUT*. We stablished a 2-fold enrichment threshold to consider a gene enriched.

Statistical Analysis

Statistical analysis was performed using GraphPad Prism V6.0. Data are presented as mean ± SEM. Comparisons were performed with a Student's t test as specified in the figure legends

Supplementary Material

Refer to Web version on PubMed Central for supplementary material.

Acknowledgments

We thank past and present members of the Laboratory of Cancer Metabolism at IDIBELL-ICO and the Department of Internal Medicine at University of Cincinnati for sharing ideas and reagents as well as their encouragement throughout the study. We are indebted to Drs. B. Ebert, N. Sonenberg, S. Volarvic and J. Warner for their critical comments of earlier drafts of this manuscript. We also thank Drs. D. Bodine, J. Boultwood, B. Ebert, S. Fumagalli, F. Guebauer, A. Narla, A. Pellagatti, M. A. Pujana, C. Onofrillo and J. Valcárcel for their advice during these studies and G. Doermann for his expertise in preparing figures. G.T. and S.C.K. are supported by Instituto de Salud Carlos III (ISCIII) grants (IIS10/00015 and II12/00002 respectively). S.C.K. is supported by the Spanish Ministry of Economy and Competitive (BFU2012-38867) grant. G.T. is supported by the Spanish Ministry of Science and Innovation (SAF2011-24967), the CIG European Commission (PCIG10-GA-2011-304160), the NIH/NCI National Cancer Institute (R01-CA158768) and the Asociación Española Contra el Cáncer (AECC GCB14-2035), ISCIII-RTICC (RD12/0036/0049), AGAUR (SGR 870) and Ministerio de Economía y Competitividad, ISCIII (PIE13/00022) grants. The Spanish Ministry grants to G.T. and S.C.K. are co-funded by FEDER – a way to build Europe – funds. A.G. was supported by an EMBO long term fellowship (ALTF 248-2012) and a shared fellowship with the IDIBELL and the Vall d'Hebron Institute of Oncology (VHIO), G. Z. R. by a Postdoctoral Fellowship from the Ciências Sem Fronteiras (249415) and J. Pelletier by a Juan de la Cierva Fellowship (FJCI-2014-20422).

References

Amaldi F, Bozzoni I, Beccari E, Pierandrei-Amaldi P. Expression of ribosomal protein genes and regulation of ribosome biosynthesis in Xenopus development. Trends in biochemical sciences. 1989; 14:175–178. [PubMed: 2672437]

Aoki K, Adachi S, Homoto M, Kusano H, Koike K, Natsume T. LARP1 specifically recognizes the 3′ terminus of poly(A) mRNA. FEBS Lett. 2013; 587:2173–2178. [PubMed: 23711370]

Avni D, Shama S, Loreni F, Meyuhas O. Vertebrate mRNAs with a 5′-terminal pyrimidine tract are candidates for translational repression in quiescent cells: characterization of the translational cis-regulatory element. Molecular and cellular biology. 1994; 14:3822–3833. [PubMed: 8196625]

Barlow JL, Drynan LF, Hewett DR, Holmes LR, Lorenzo-Abalde S, Lane AL, Jolin HE, Pannell R, Middleton AJ, Wong SH, et al. A p53-dependent mechanism underlies macrocytic anemia in a mouse model of human 5q- syndrome. Nature medicine. 2010; 16:59–66.

Bursac S, Brdovcak MC, Pfannkuchen M, Orsolic I, Golomb L, Zhu Y, Katz C, Daftuar L, Grabusic K, Vukelic I, et al. Mutual protection of ribosomal proteins L5 and L11 from degradation is essential for p53 activation upon ribosomal biogenesis stress. Proceedings of the National Academy of Sciences of the United States of America. 2012; 109:20467–20472. [PubMed: 23169665]

Carvalho BS, Irizarry RA. A framework for oligonucleotide microarray preprocessing. Bioinformatics. 2010; 26:2363–2367. [PubMed: 20688976]

Damgaard CK, Lykke-Andersen J. Translational coregulation of 5′TOP mRNAs by TIA-1 and TIAR. Genes & development. 2011; 25:2057–2068. [PubMed: 21979918]

Donati G, Peddigari S, Mercer CA, Thomas G. 5S Ribosomal RNA Is an Essential Component of a Nascent Ribosomal Precursor Complex that Regulates the Hdm2-p53 Checkpoint. Cell reports. 2013; 4:87–98. [PubMed: 23831031]

Dutt S, Narla A, Lin K, Mullally A, Abayasekara N, Megerdichian C, Wilson FH, Currie T, Khanna-Gupta A, Berliner N, et al. Haploinsufficiency for ribosomal protein genes causes selective activation of p53 in human erythroid progenitor cells. Blood. 2010

Ebert BL, Pretz J, Bosco J, Chang CY, Tamayo P, Galili N, Raza A, Root DE, Attar E, Ellis SR, et al. Identification of RPS14 as a 5q- syndrome gene by RNA interference screen. Nature. 2008; 451:335–339. [PubMed: 18202658]

Flygare J, Karlsson S. Diamond-Blackfan anemia: erythropoiesis lost in translation. Blood. 2007; 109:3152–3154. [PubMed: 17164339]

Fonseca BD, Zakaria C, Jia JJ, Graber TE, Svitkin Y, Tahmasebi S, Healy D, Hoang HD, Jensen JM, Diao IT, et al. La-related Protein 1 (LARP1) Represses Terminal Oligopyrimidine (TOP) mRNA Translation Downstream of mTOR Complex 1 (mTORC1). The Journal of biological chemistry. 2015; 290:15996–16020. [PubMed: 25940091]

Fumagalli S, Di Cara A, Neb-Gulati A, Natt F, Schwemberger S, Hall J, Babcock GF, Bernardi R, Pandolfi PP, Thomas G. Absence of nucleolar disruption after impairment of 40S ribosome biogenesis reveals an rpL11-translation-dependent mechanism of p53 induction. Nature cell biology. 2009; 11:501–508. [PubMed: 19287375]

Fumagalli S, Ivanenkov VV, Teng T, Thomas G. Suprainduction of p53 by disruption of 40S and 60S ribosome biogenesis leads to the activation of a novel G2/M checkpoint. Genes & development. 2012; 26:1028–1040. [PubMed: 22588717]

Gentilella A, Khalili K. BAG3 expression in glioblastoma cells promotes accumulation of ubiquitinated clients in an Hsp70-dependent manner. The Journal of biological chemistry. 2011; 286:9205–9215. [PubMed: 21233200]

Gentilella A, Passiatore G, Deshmane S, Turco MC, Khalili K. Activation of BAG3 by Egr-1 in response to FGF-2 in neuroblastoma cells. Oncogene. 2008; 27:5011–5018. [PubMed: 18469860]

Gentilella A, Thomas G. Cancer biology: The director's cut. Nature. 2012; 485:50–51. [PubMed: 22552093]

Gismondi A, Caldarola S, Lisi G, Juli G, Chellini L, Iadevaia V, Proud CG, Loreni F. Ribosomal stress activates eEF2K-eEF2 pathway causing translation elongation inhibition and recruitment of terminal oligopyrimidine (TOP) mRNAs on polysomes. Nucleic acids research. 2014; 42:12668–12680. [PubMed: 25332393]

Granneman S, Tollervey D. Building ribosomes: even more expensive than expected? Current biology: CB. 2007; 17:R415–417. [PubMed: 17550767]

Holzel M, Orban M, Hochstatter J, Rohrmoser M, Harasim T, Malamoussi A, Kremmer E, Langst G, Eick D. Defects in 18 S or 28 S rRNA processing activate the p53 pathway. The Journal of biological chemistry. 2010; 285:6364–6370. [PubMed: 20056613]

Hsieh AC, Liu Y, Edlind MP, Ingolia NT, Janes MR, Sher A, Shi EY, Stumpf CR, Christensen C, Bonham MJ, et al. The translational landscape of mTOR signalling steers cancer initiation and metastasis. Nature. 2012; 485:55–61. [PubMed: 22367541]

Jefferies HB, Fumagalli S, Dennis PB, Reinhard C, Pearson RB, Thomas G. Rapamycin suppresses 5′TOP mRNA translation through inhibition of p70s6k. Embo J. 1997; 16:3693–3704. [PubMed: 9218810]

Jefferies HB, Reinhard C, Kozma SC, Thomas G. Rapamycin selectively represses translation of the "polypyrimidine tract" mRNA family. Proceedings of the National Academy of Sciences of the United States of America. 1994; 91:4441–4445. [PubMed: 8183928]

Keene JD, Komisarow JM, Friedersdorf MB. RIP-Chip: the isolation and identification of mRNAs, microRNAs and protein components of ribonucleoprotein complexes from cell extracts. Nature protocols. 2006; 1:302–307. [PubMed: 17406249]

Lam YW, Lamond AI, Mann M, Andersen JS. Analysis of nucleolar protein dynamics reveals the nuclear degradation of ribosomal proteins. Current biology: CB. 2007; 17:749–760. [PubMed: 17446074]

McGowan KA, Pang WW, Bhardwaj R, Perez MG, Pluvinage JV, Glader BE, Malek R, Mendrysa SM, Weissman IL, Park CY, et al. Reduced ribosomal protein gene dosage and p53 activation in low-risk myelodysplastic syndrome. Blood. 2011; 118:3622–3633. [PubMed: 21788341]

Meyuhas O, Kahan T. The race to decipher the top secrets of TOP mRNAs. Biochimica et biophysica acta. 2015; 1849:801–811. [PubMed: 25234618]

Pellagatti A, Boultwood J. Recent Advances in the 5q- Syndrome. Mediterranean journal of hematology and infectious diseases. 2015; 7:e2015037. [PubMed: 26075044]

Pellagatti A, Hellstrom-Lindberg E, Giagounidis A, Perry J, Malcovati L, Della Porta MG, Jadersten M, Killick S, Fidler C, Cazzola M, et al. Haploinsufficiency of RPS14 in 5q- syndrome is associated with deregulation of ribosomal- and translation-related genes. British journal of haematology. 2008; 142:57–64. [PubMed: 18477045]

Pellagatti A, Marafioti T, Paterson JC, Barlow JL, Drynan LF, Giagounidis A, Pileri SA, Cazzola M, McKenzie AN, Wainscoat JS, et al. Induction of p53 and up-regulation of the p53 pathway in the human 5q- syndrome. Blood. 2010; 115:2721–2723. [PubMed: 20360478]

Pierandrei-Amaldi P, Beccari E, Bozzoni I, Amaldi F. Ribosomal protein production in normal and anucleolate Xenopus embryos: regulation at the posttranscriptional and translational levels. Cell. 1985; 42:317–323. [PubMed: 4016954]

Schneider RK, Schenone M, Ferreira MV, Kramann R, Joyce CE, Hartigan C, Beier F, Brummendorf TH, Germing U, Platzbecker U, et al. Rps14 haploinsufficiency causes a block in erythroid differentiation mediated by S100A8 and S100A9. Nature medicine. 2016; 22:288–297.

Signer RA, Magee JA, Salic A, Morrison SJ. Haematopoietic stem cells require a highly regulated protein synthesis rate. Nature. 2014; 509:49–54. [PubMed: 24670665]

Sonenberg N, Hinnebusch AG. Regulation of translation initiation in eukaryotes: mechanisms and biological targets. Cell. 2009; 136:731–745. [PubMed: 19239892]

Sridhar K, Ross DT, Tibshirani R, Butte AJ, Greenberg PL. Relationship of differential gene expression profiles in CD34+ myelodysplastic syndrome marrow cells to disease subtype and progression. Blood. 2009; 114:4847–4858. [PubMed: 19801443]

Tcherkezian J, Cargnello M, Romeo Y, Huttlin EL, Lavoie G, Gygi SP, Roux PP. Proteomic analysis of cap-dependent translation identifies LARP1 as a key regulator of 5′TOP mRNA translation. Genes & development. 2014; 28:357–371. [PubMed: 24532714]

Teng T, Thomas G, Mercer CA. Growth control and ribosomopathies. Current opinion in genetics & development. 2013; 23:63–71. [PubMed: 23490481]

Thoreen CC, Chantranupong L, Keys HR, Wang T, Gray NS, Sabatini DM. A unifying model for mTORC1-mediated regulation of mRNA translation. Nature. 2012; 485:109–113. [PubMed: 22552098]

Volarevic S, Stewart MJ, Ledermann B, Zilberman F, Terracciano L, Montini E, Grompe M, Kozma SC, Thomas G. Proliferation, but not growth, blocked by conditional deletion of 40S ribosomal protein S6. Science. 2000; 288:2045–2047. [PubMed: 10856218]

Wang L, Fidler C, Nadig N, Giagounidis A, Della Porta MG, Malcovati L, Killick S, Gattermann N, Aul C, Boultwood J, et al. Genome-wide analysis of copy number changes and loss of heterozygosity in myelodysplastic syndrome with del(5q) using high-density single nucleotide polymorphism arrays. Haematologica. 2008; 93:994–1000. [PubMed: 18508791]

Warner JR. In the absence of ribosomal RNA synthesis, the ribosomal proteins of HeLa cells are synthesized normally and degraded rapidly. Journal of molecular biology. 1977; 115:315–333. [PubMed: 592369]

Woolford JL Jr, Baserga SJ. Ribosome biogenesis in the yeast Saccharomyces cerevisiae. Genetics. 2013; 195:643–681. [PubMed: 24190922]

Yamashita R, Suzuki Y, Takeuchi N, Wakaguri H, Ueda T, Sugano S, Nakai K. Comprehensive detection of human terminal oligo-pyrimidine (TOP) genes and analysis of their characteristics. Nucleic acids research. 2008; 36:3707–3715. [PubMed: 18480124]

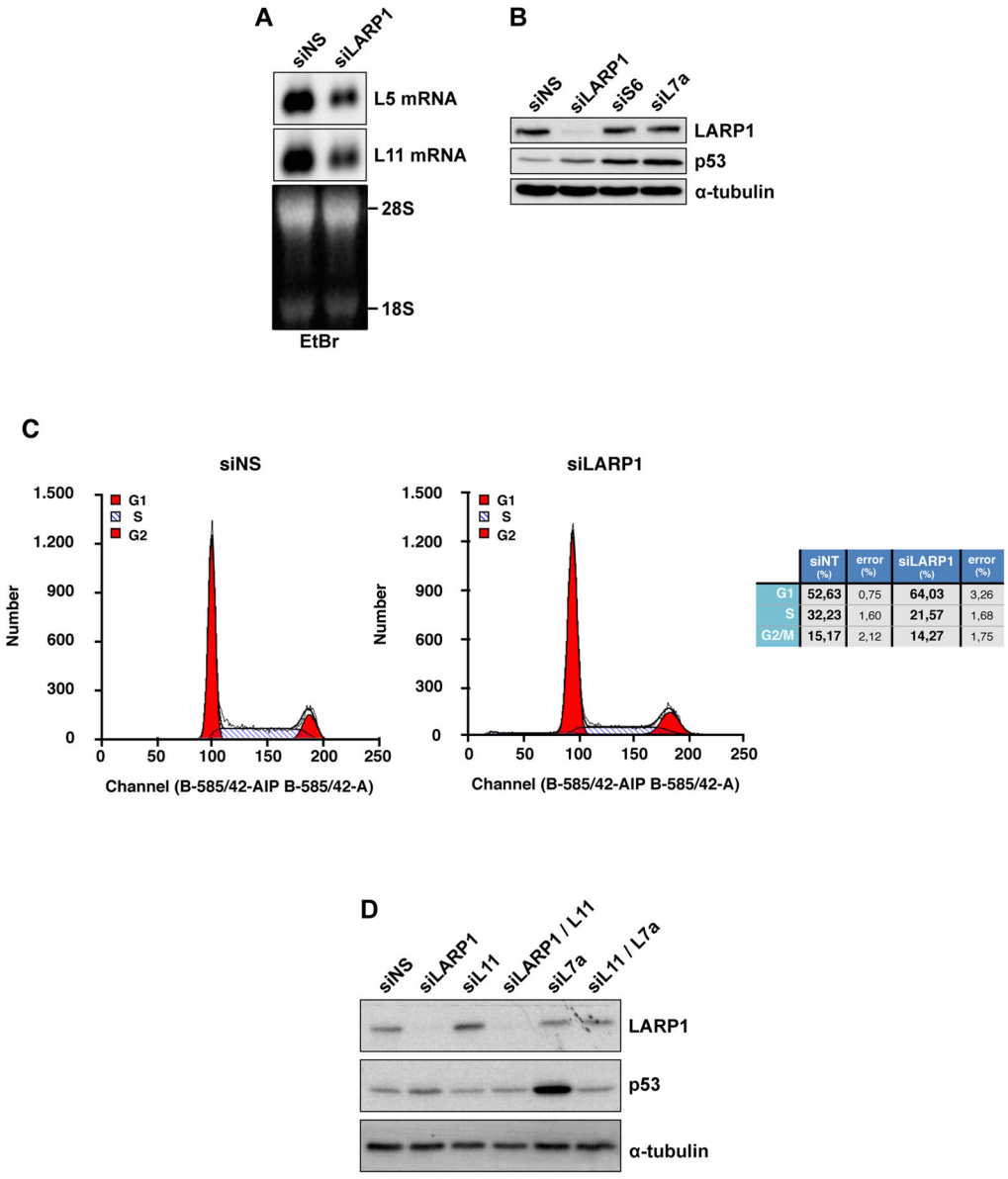

Figure 1. Effect of LARP1 depletion on p53 stabilization and cell cycle progression

(**A**) Total RNA extracted from HCT116 cells transfected with siLARP1 or siNS for 48h was used for northern blot analysis and hybridized with DNA oligos complementary to either RPL5 or RPL11 mRNAs. (**B**) HCT116 cells were transfected with the indicated siRNAs. Whole cell lysates were analyzed by western blot analysis for the indicated proteins with the corresponding antibodies. Data is representative of four independent experiments (**C**) HCT116 cells treated as in panel **A** were subjected to propidium iodide staining and FACS analysis. Data is representative of three independent experiments. (**D**) HCT116 cells were transfected with siLARP1 or siNS for 24h, followed by a second transfection with siRPL7a and/or siRPL11 for an additional 24h. Data is representative of three independent experiments. α-tubulin serves as loading control.

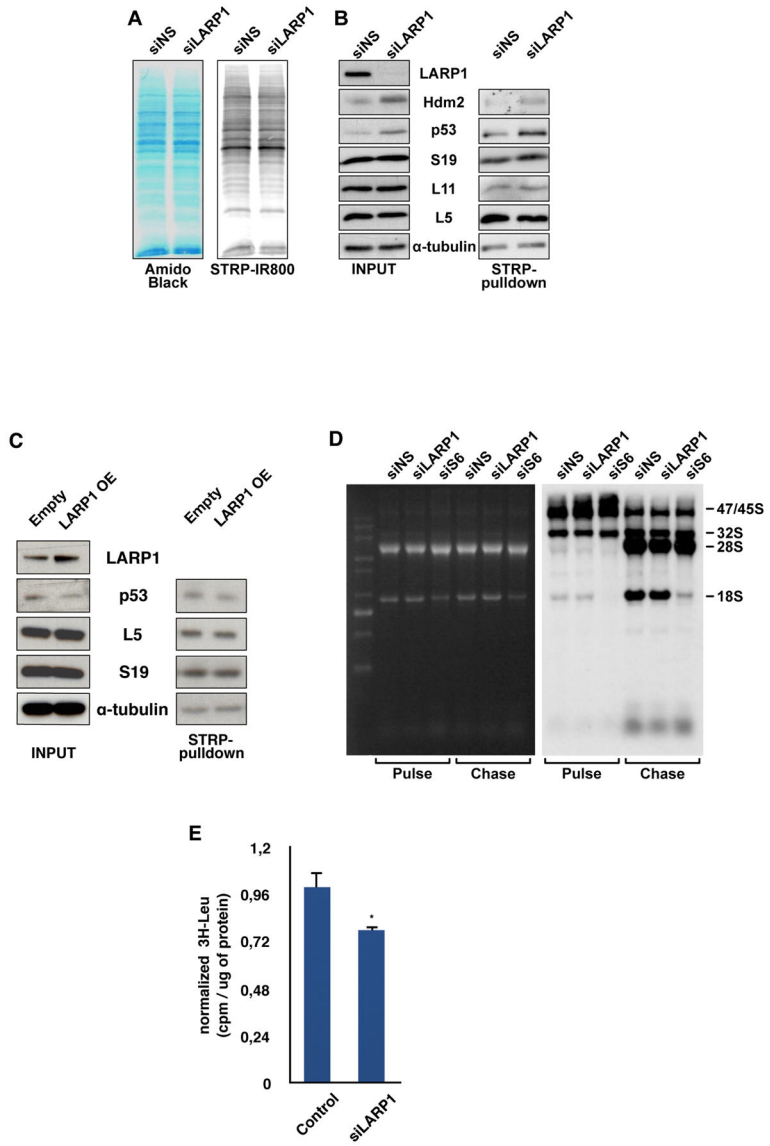

Figure 2. Effect of LARP1 depletion on newly synthesized proteins and ribosomes

(**A**) HCT116 cells were transfected with siLARP1 or siNS for 48h and *de novo* synthesized proteins were labelled by alkyne-biotine click-iT reaction (see Experimental Procedures). The labeling efficiency of the experimental conditions was evaluated by western blotting of biotinylated proteins and hybridizing the membrane with streptavidin-IRDye800. The intensity of the signals was detected using an infrared scanner and was compared to Amido Black membrane staining. (**B**) Total cell extracts (INPUT) and nascent proteins from INPUTs, pulled-down using streptavidin-agarose beads (STRP-pulldown), were resolved by western blot analysis with the indicated antibodies. Data is representative of three independent experiments (**C**) HCT116 were transfected with a plasmid encoding for LARP1 protein. 48h after transfection cells were labeled and processed as in panel A. (**D**) HCT116 cells were treated with the indicated siRNAs for 48h or siS6 for 24h. Cells were pulsed with ^{3}H-Uridine and chased with non-radioactive uridine. Total RNAs were extracted and

resolved by Northern blot analysis and exposed in presence of emission enhancer. This experiment is representative of 3 independent experiments. (**E**) Quantification of the global protein synthesis rate by the incorporation of ^{3}H-leucine into total protein (Data are means +/− s.e.m. n=3) *p<0.01 calculated by Student's t test.

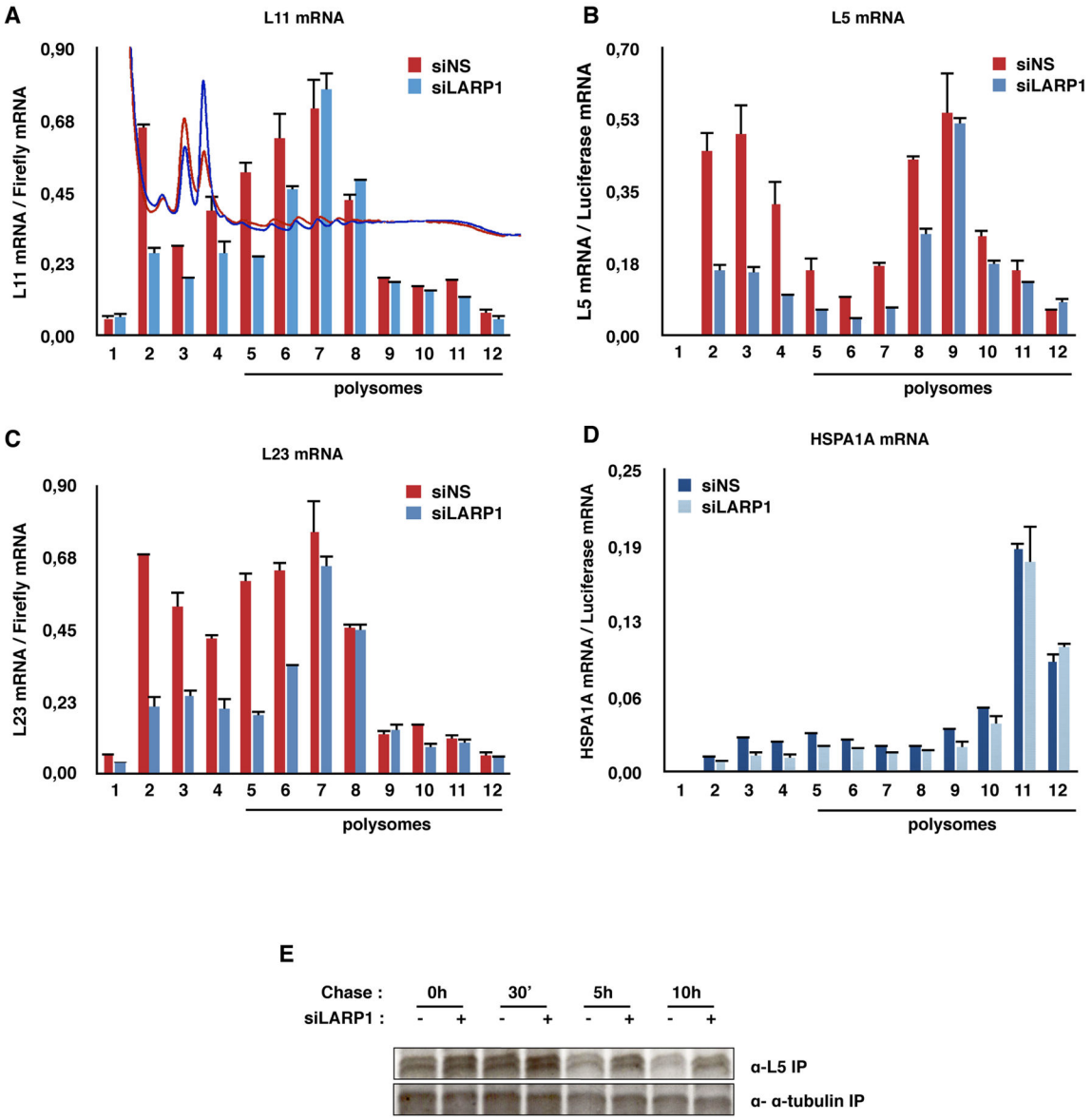

Figure 3. Analysis of the distribution of RPL11 and RPL23 mRNAs on polysome gradients

(**A**) Polysome profiles of HCT116 cells transfected with siLARP1 or siNS for 48h. The polysome profile is representative of three independent experiments. RNA analyses were carried out as described in Experimental Procedures. (**A**) RPL11 mRNA, (**B**) RPL5, (**C**) RPL23 and (**D**) HSPA1A mRNAs distribution across the gradient was evaluated in each fraction by RT-qPCR as described in Experimental Procedures. Error bars represent replicates for RT-qPCR (for RPL11 three more replicates of this experiment are shown in Fig S3A and Fig 6C) (**E**) HCT116 cells were transfected with the indicated siRNAs for 48h, metabolically labeled with ^{35}S-Met/Cys for 2h in DMEM 10% FBS, and chased for the indicated times with non-radioactive DMEM 10% FBS. Equal amounts of whole protein lysates in each condition were subjected to immunoprecipitation with α-L5 or α-α-tubulin

antibodies. Immunocomplexes were analyzed by SDS-PAGE and visualized by autoradiography.

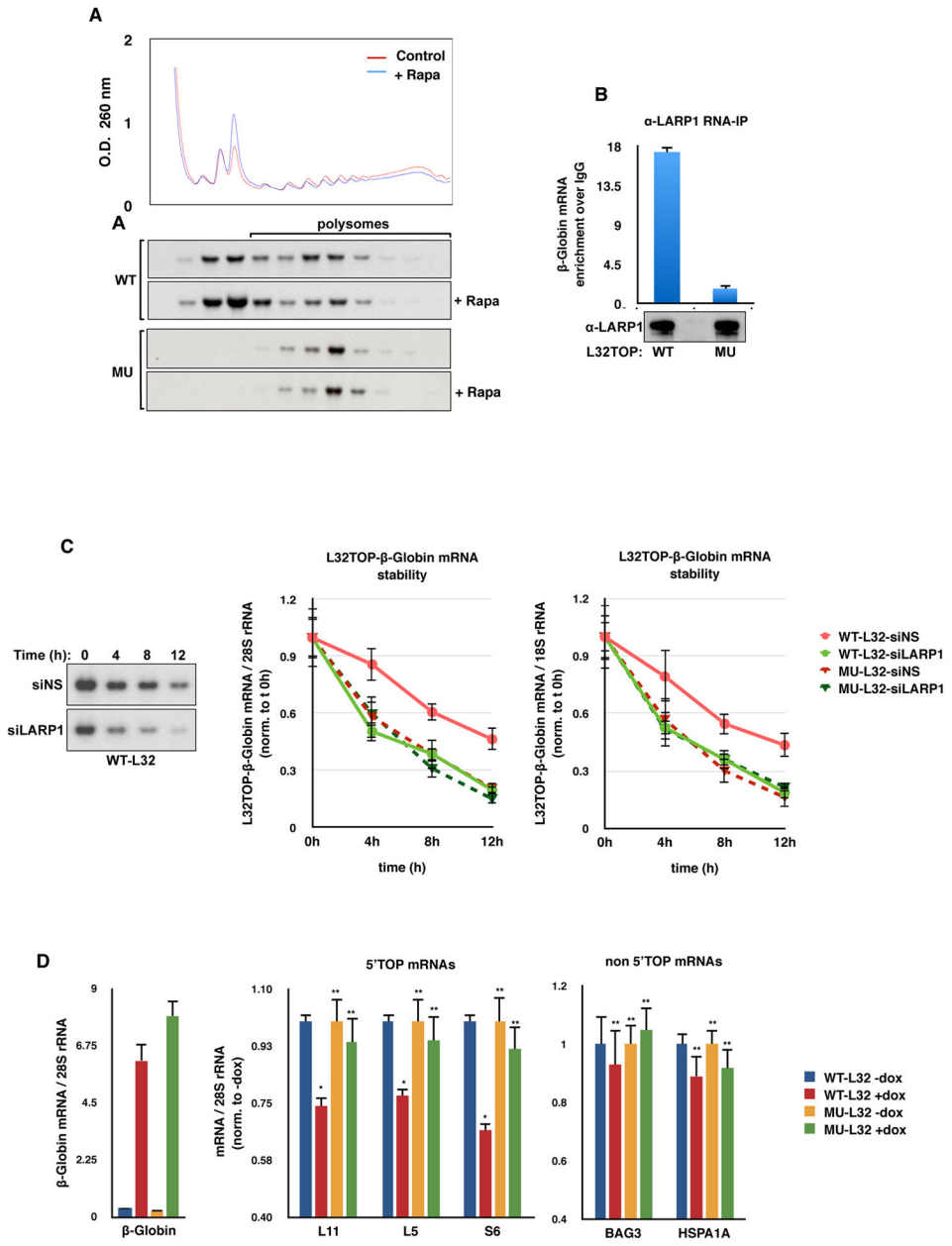

Figure 4. The effect of LARP1 depletion on the half-life of 5′TOP mRNA reporters

(**A**) Effect of rapamycin treatment on the polysomal distribution of WT-RPL32- and MU-RPL32-β-globin reporter transcripts. Following fractionation and purification, RNA was probed by northern blot with an oligo complementary to β-Globin mRNA. (**B**) LARP1 immunoprecipitation from cells expressing WT-RPL32- or MU-RPL32-β-Globin mRNAs. Top Panel: LARP1-immunoprecipitated complexes were RNA purified, and analyzed by RT-qPCR. The fold enrichment of β-globin cDNA was measured as compared to complexes immunoprecipitated by an IgG control antibody. Bottom panel: 20% of immunoprecipitated complexes were subjected to western blot analysis (**C**) Determination of WT-RPL32- and MU-RPL32-β-Globin mRNA stability upon LARP1 depletion. Tet-ON/Doxycycline-

inducible WT-RPL32- or MU-RPL32-β-globin reporters stably transfected HCT116 cells were induced with doxycyline for 16h, followed by siRNA transfection for 24h. Cells were deprived of doxycycline and harvested at the indicated times. Equal amounts of total RNA were analyzed by northern blot and probed for β-globin reporter (left panel). Total RNA from biological replicates of the same samples were analyzed for β-globin mRNA by RT-qPCR and 28S rRNA (middle panel) or 18S rRNA (right panel) were used as internal controls. All time points were normalized to time 0h (right panel). $P<0.05$ by Student's two-tailed t-test, mean and s.e.m. shown (n=3) (**D**) HCT116 Tet-ON stable clones were transfected with Doxycyline-inducible WT- or MU-RPL32-β-globin reporter plasmids, then treated with doxycycline for 24h. Total RNA was analyzed by RT-qPCR and the indicated mRNAs were measured and normalized by 28S rRNA. Data are means +/− s.e.m. n=2. * $p<0.01$, ** $p<0.05$ by t Student's.

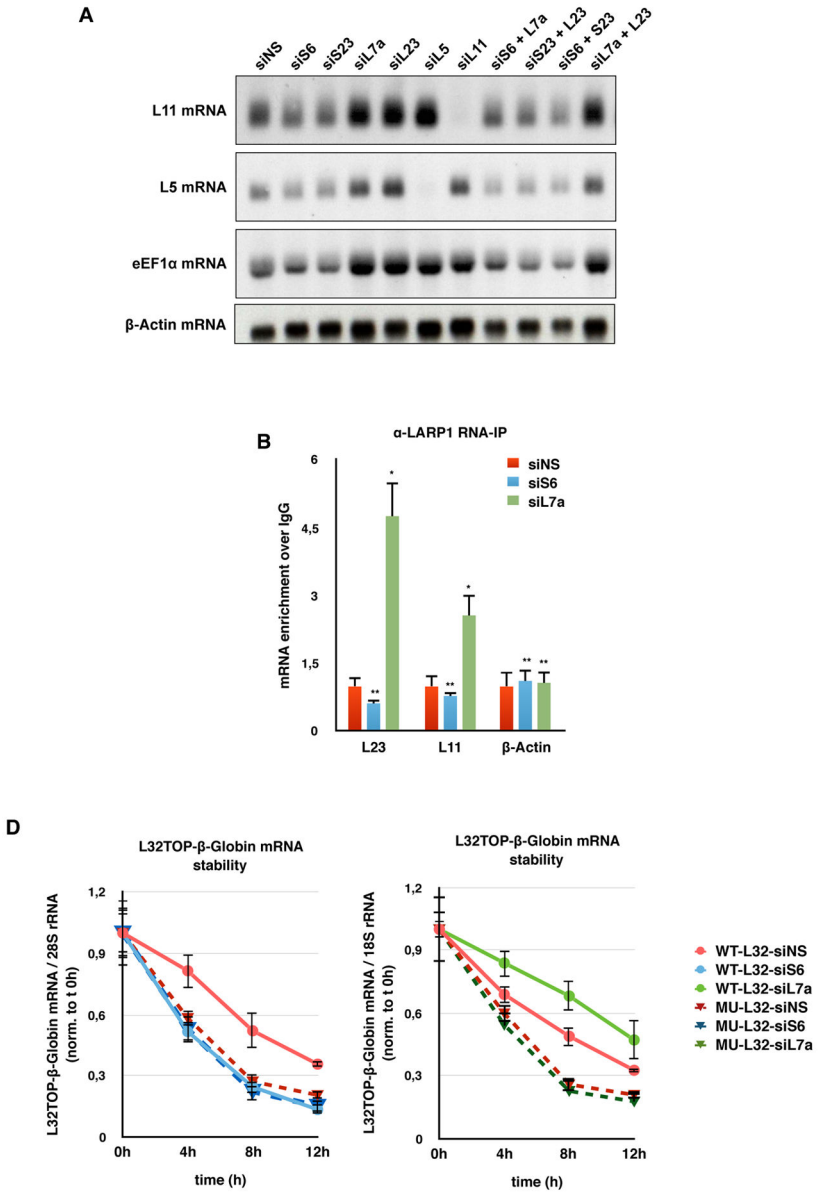

Figure 5. 40S ribosomes control 5′TOP mRNA stability

(**A**) HCT116 cells were treated with siRNA targeting the indicated RPs for 48h. Equal amounts of whole cell extracts, based on total RNA, were resolved on northern blots probed for RPL11, RPL5, eEF1α and β-actin mRNAs.(**B**) LARP1 was immunoprecipitated from cells transfected with the indicated siRNA for 24 h and the presence of endogenous 5′TOP mRNAs, RPL23 and RPL11, or a non-TOP mRNAs, β-Actin, were determined by RT-qPCR. Data are mean +/− s.e.m. n=3 * $p<0.01$, **$p<0.05$ by t Student's. (**C**) WT-RPL32 or MU-RPL32-β-globin mRNA stability was determined as in Figure 4C. β-globin mRNA was normalized by 28S rRNA in siNS and siS6 transfected cells (left panel) or by 18S rRNA in siNS and siL7a-transfected cells (right panel). $p<0.05$ by Student's two-tailed t-test, mean and s.e.m. shown (n=3).

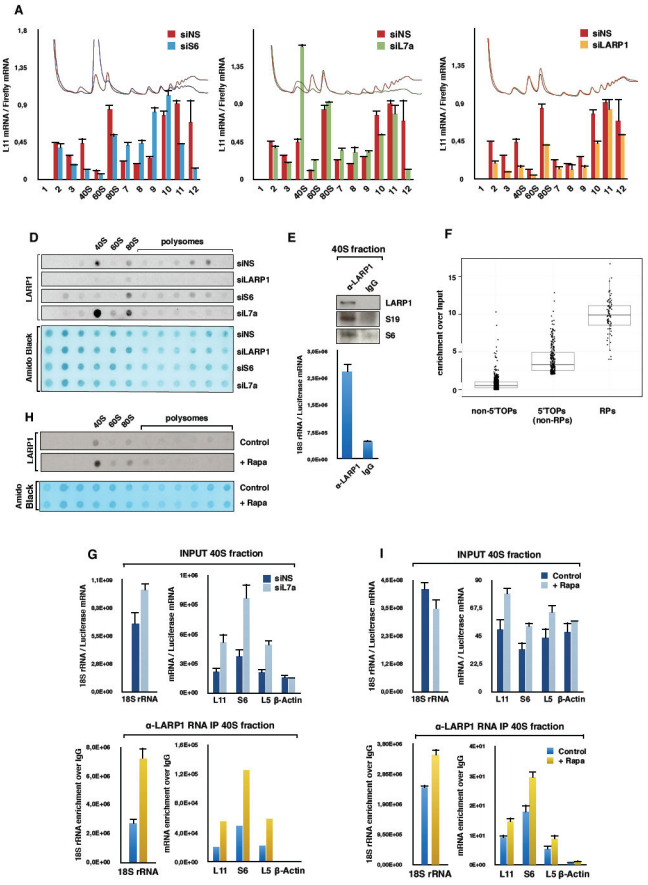

Figure 6. Native 40S ribosomes control 5′TOP mRNA stability

Polysome distribution from HCT116 cells transfected with the indicated siRNAs for 40 h **A**, **B** and **C**. (**A**) The distribution of RPL11 mRNA on a 10–50% sucrose gradient following siRNA depletion of RPS6, (**B**) RPL7a or (**C**) LARP1 after 40 h of transfection. Data are means +/− s.e.m. n=2. (**D**) Protein extracted from the 20% of polysome profiles fractions shown in panel **A**, **B** and **C** were (upper panel) subjected to dot blot analysis with an α-LARP1 antibody after staining with amido black (lower panel). Data is representative of 3 independent experiments. (**E**) Immunoprecipitation of LARP1 from 40S fraction isolated from growing HCT116 cells. Immunocomplexes were analyzed by western blot and probed with α-LARP1, α-S6 and α-S19 antibodies. 20% of immunoprecipitates were spiked with Luciferase mRNA external control, RNA purified and 18S rRNA and Luciferase mRNA were measured by RT-qPCR. (n=4, p<0.01) (**F**) Boxplot showing mRNA enrichment over inputs in the 40S peak immunoprecipitated with the LARP1 antibody and subjected to RNA-seq. Left, non-5′-TOP boxplot of 680 genes whose mRNAs are lacking a 5′-TOP. Middle, 5′-TOP boxplot of 236 genes, excluding RP genes, whose mRNAs contain a 5′TOP. Right, boxplot of 74 RP genes. T-tests on log2 fold enrichment values show all groups have significant differences, with a p-value < 2.2E-16. 5′TOP transcripts considered in the analysis were isoforms starting with a C and showing a minimum of 4 consecutive pyrimidines (See Table S1). (**G**) α-LARP1 immunoprecipitation from 40S fraction obtained from siNS or siL7a transfected cells, as described in **E**. The indicated mRNAs were

measured by RT-qPCR in the 40S INPUT fractions (left panel) and in the α-LARP1 immunocomplexes enriched over IgG control IP (right panel). Data are mean −/+ s.e.m. n=4 for siNS and n=2 for siL7a. $p<0.01$ calculated by Student's t test. (**H**) Immunoprecipitation of LARP1 form 40S fractions isolated from growing cells or cells treated with 40nM Rapamycin for 5h. RT-qPCR analysis was carried out as described in **G**. (**I**) 20% of polysomal lysates isolated in **H** were subjected to dot-blot analysis as in **D**. This data is representative of two experiments.

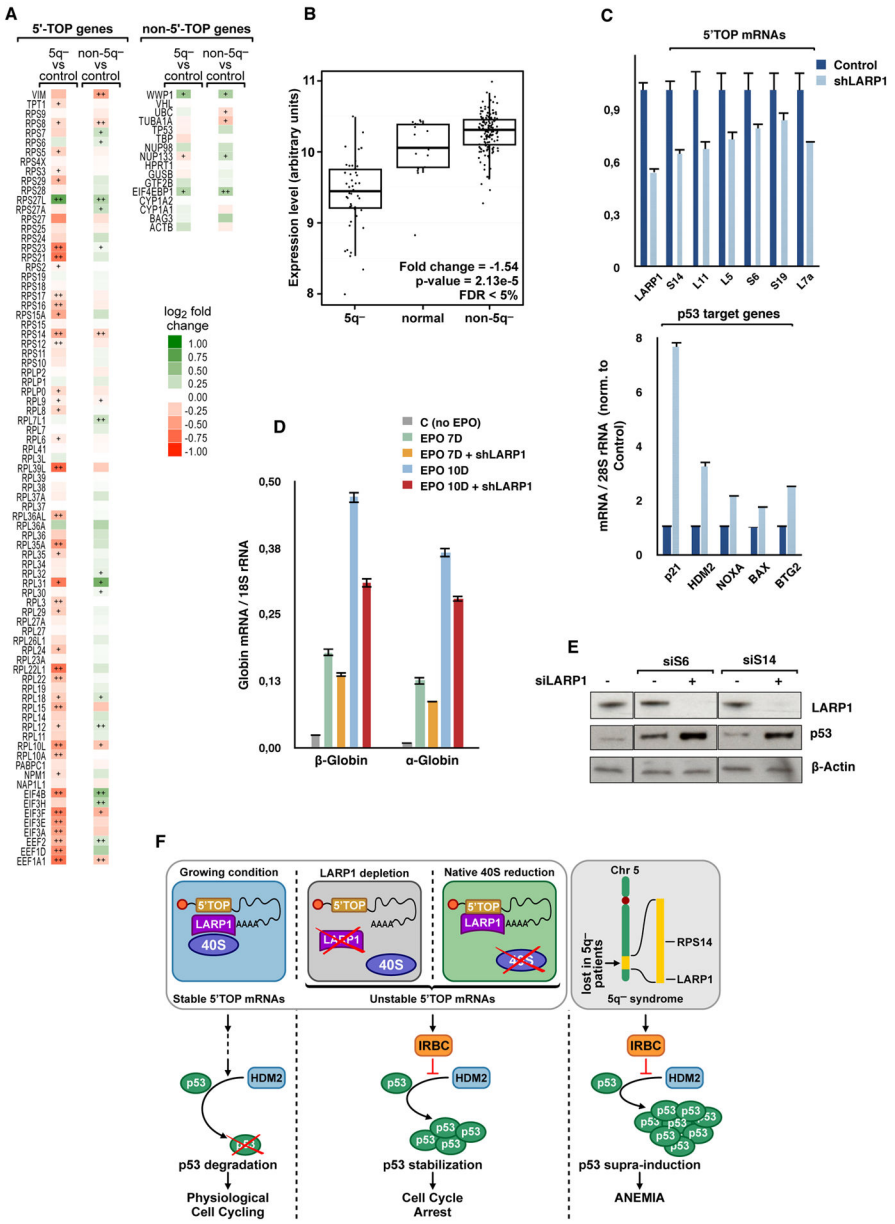

Figure 7. Loss of LARP1 and 5′TOP mRNAs in *5q*⁻ patients and CD34+ cells

(**A**) Heat map representation of $\log_2$ fold change of a 5′TOP mRNAs panel, including RPs of *5q*⁻ and non *5q*⁻ MDS patients versus controls (left) and a panel of non-5′TOP mRNAs for both groups (right). (+): significant fold changes; (++) those significant genes with FDR < 5%. (**B**) LARP1 expression levels in CD34+ cells from a cohort of 47 *5q*⁻ patients and 136 non *5q*⁻ patients compared to 17 healthy individuals. (**C**) CD34+ cells from healthy donors were transduced with shControl or shLARP1 lentiviral particles and subjected to erythroid lineage differentiation protocol (see Experimental Procedures). Total RNA extracted at 7 days after transduction were analyzed by RT-qPCR. Total level of LARP1 and six RP mRNAs (left panel) and p53 target genes (right panel) were determined. (**D**) CD34+ cells from healthy donors treated as in C were analyzed at 7 days or 10 days after transduction by

RT-qPCR. (**E**) HCT116 cells transfected with siLARP1 or siNS for 24 h and followed by siS14 or siS6 treatment for an additional 24h. Protein lysates were analyzed on western blots for the indicated proteins. (**F**) Left hand panel, LARP1 mediates the interaction between native 40S ribosomes and 5′TOP mRNAs. Middle panels, loss of either LARP1 or native 40S subunits leads to activation of the IRBC and stabilization of p53. Right hand panel, 5q-syndrome leads to a reduction of both LARP1 and native 40S ribosomes, hyperactivation of IRBC and p53, resulting in anemia.